ARTICLES

A Simple Multichromophore Design for Energy Transfer in Distyrylbenzenes with Pyrene Pendants

Cesar A. Sierra[†] **and Paul M. Lahti***

Department of Chemistry, University of Massachusetts, Amherst, Massachusetts 01003

Received: January 25, 2006; In Final Form: August 25, 2006

A set of Don → Acc ← Don multichromophores was synthesized based on a simple design with two pyrene donors (absorbing antennae) connected to a bis-1,4-(3,4,5-trimethoxystyryl)benzene core acceptor using various flexible, nonconjugated tethers. Excitation of the pyrene donors at 276 nm in solution yields near exclusive emission from the core chromophore at 445−450 nm, with energy transfer efficiencies up to 92%, far better than achieved with simple mixtures. The simple tethering design imposes a high "local" concentration of the pyrene near the acceptor core unit that is maintained even at very low multichromophore concentrations. Solvent effects on absorption and emission spectra are very small, except in cases where a π-conjugating O−C═O moiety of the tethering group is directly attached to the core chromophore, rather than being placed in the middle of the tether. Energy transfer in the systems is effective due to good donor−acceptor energy matching. The optimal energy transfer efficiency was achieved using an eight-atom flexible linker.

Introduction

There is much interest in understanding and controlling intermolecular and intramolecular energy transfer in organic conjugated molecules and polymers, as basic research concerning photophysics and as part of the development of photonic materials. In multichromophoric molecules, one can design energy absorption by one or more "antenna" chromophores, which can then transfer their energy to an acceptor chromophore that will in turn photoluminescence.[1] The plethora of available chromophores and means of connecting them provides great scope for systems with widely variable energetic and structural characteristics.

We have studied the electronic spectroscopy of polyphenylenevinylenes (PPVs) and related systems with controlled chromophore conjugation lengths, especially in segmented block copolymers,[2] that alternate conjugated chromophores with nonconjugated solubilizing polymethylene chains. Since the segmented copolymers have multiple chromophores held in proximity, energy transfer between the chromophores can influence their luminescence behavior, especially in systems having a random distribution with different chromophores. The behavior of such segmented multichromophoric systems bears investigation by comparison to more-studied copolymers that incorporate different chromophoric units. It is easier to understand such structure property relationships by constructing simpler analogues with better-defined structures.

In this article, we report the synthesis and solution photophysical characterization of multichromophoric molecules **1**−**4**, with comparison to the related, segmented copolymer **5**. The molecular systems all have well-defined structures assembled using simple units: pyrene antenna chromophores attached to a central *para*-distyrylbenzene (2.5-oligo-PPV) core emitter with variable flexible tether groups to form a Don → Acc ← Don triad. By comparison, the segmented copolymer incorporates similar structural units that are connected by octamethylene groups, further linking all the chromophores in relative proximity to one another. This basic set of molecules allows an initial evaluation of pyrene → distyrylbenzene as an energy transfer set for blue emission, using a synthetically simple proximity tethering strategy that allows wide variation of maximum distances and (eventually) variation of the tether structure itself for changes in rigidity and polarity.

Experimental Section

General Methods. All solvents were used as received. Polymer molecular weights were measured by gel permeation chromatography in tetrahydrofuran and referenced against linear polystyrene standards using a three-column system (Polymer Laboratories 300 × 7.5 mm, 2 mixed-D, 50 Å), a Knauer K-501 pump with a K-2301 refractive index detector, and a K-2600 UV detector (395 nm). Relative quantum yields (ϕ_{fl}) were measured using quinine sulfate in 0.10 M H_2SO_4 as a standard ($\phi_{fl} = 0.546$), according to the procedure of Chen et al.[3]

Materials. All compounds were synthesized from commercially available precursors as shown in Scheme 1. Full details of the synthetic methodologies and characterization of intermediates are given in the Supporting Information. Characterization of the multichromophores and appropriate model compounds is given below.

(*E*,*E*)-2,5-Bis(2-[4-(1-pyrenyl)butoxy]ethoxy)-1,4-bis((3,4,5-trimethoxystyryl)-benzene (1). Mp: 65−71 °C. HRMS (FAB, *m*/*z*): anal. calcd for $C_{72}H_{70}O_{10}$, 1094.4969; found, 1094.5305. UV−vis (chloroform, λ_{max}/nm [ϵ]): 245 [50700], 269 [22600],

* To whom correspondence should be addressed. E-mail: lahti@chem.umass.edu.

[†] Present address: Departamento de Quimica, Universidad Nacional de Colombia, AA 14490, Bogata, Columbia.

10.1021/jp060543g CCC: $33.50
Published on Web 10/17/2006

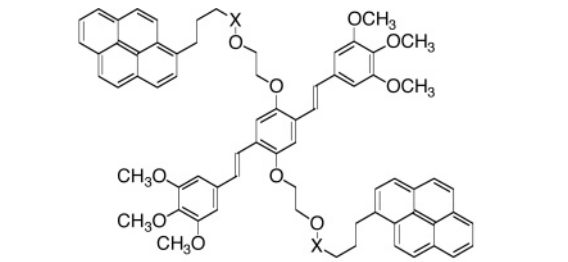

1 X = CH_2
2 X = CO

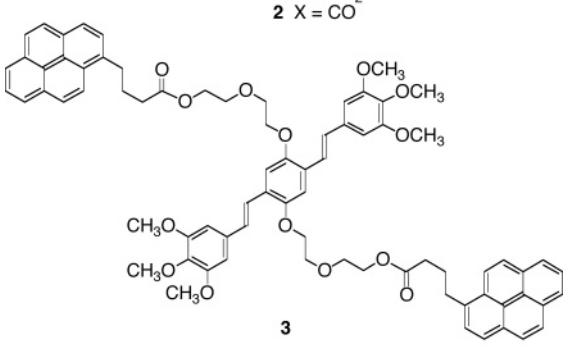

3

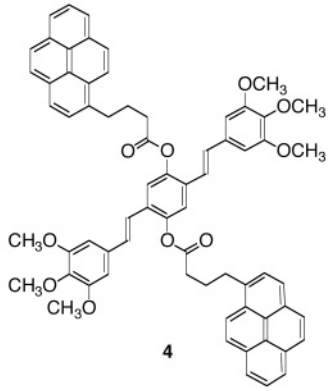

4

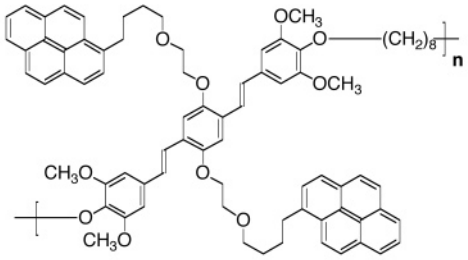

5

276 [36300], 330 [27900], 346 [37500], 387 broad [10300]. ^{1}H NMR ($CDCl_3$): δ 1.83 (m, 4 H), 1.94 (m, 4 H), 3.32 (t, 4 H, J = 8 Hz), 3.64 (t, 4 H, J = 6 Hz), 3.83 (overlapping s plus t, 22 H), 4.22 (t, 4 H, J = 5 Hz), 6.68 (s, 4 H), 7.01 (d, 2 H, J = 16 Hz), 7.34 (d, 2 H, J = 16 Hz), 7.14 (s, 2 H), 7.77 (d, 2 H, J = 8 Hz), 7.90−8.24 (m, 18 H). ^{13}C NMR (400 MHz, $CDCl_3$): 28.33, 29.69, 33.16, 56.04, 60.95, 69.33, 69.53, 71.44, 103.67, 122.82, 123.35, 124.64, 124.74, 124.78, 124.98, 125.74, 126.52, 127.17, 127.48, 129.10, 130.86, 131.86, 136.62, 153.30.

(*E*,*E*)-2,5-Bis(2-[4-(1-pyrenyl)butyryloxy]ethoxy)-1,4-bis-[2-(3,4,5-trimethoxy styryl)-benzene (2). Mp: 162−164 °C. HRMS (FAB, *m*/*z*): anal. calcd for $C_{72}H_{66}O_{12}$, 1122.4554; found, 1122.4496. ^{1}H NMR ($CDCl_3$): δ 2.15 (m, 4 H), 2.46 (t, 4 H, J = 7 Hz), 3.28 (t, 4 H, J = 7 Hz), 3.84 (s, 4 H), 3.86 (s, 14 H), 4.22 (t, 4 H, J = 5 Hz), 4.55 (t, 4 H, J = 5 Hz), 6.72 (s, 4 H), 6.95 (d, 2 H, J = 16 Hz), 7.04 (s, 2H), 7.33 (d, 2 H, J = 16 Hz), 7.72 (d, 2 H, J = 8 Hz), 7.92 (m, 10 H), 8.12 (m, 6 H). ^{13}C NMR ($CDCl_3$): 26.92, 32.84, 34.20, 56.43, 61.27, 67.95, 104.02, 121.95, 122.59, 123.45, 125.05, 125.18, 125.28, 126.10, 126.97, 127.23, 127.47, 127.61, 127.74, 128.95, 129.69, 130.20, 131.13, 131.66, 133.70, 135.72, 138.30, 151.09, 153.68, 173.64. FTIR (KBr pellet, cm^{-1}): 3035, 2934, 1735, 1580, 1507, 1419, 1322, 1244, 1127, 1005, 962, 844. UV−vis (THF, λ_{max}/nm [ϵ]): 243 [94600], 264 [47200], 276 [70100], 327 [75000], 343 [97000], 397 [48200].

(*E*,*E*)-2,5-Bis(2-[2-(4-[1-pyrenyl]butyryloxy)-ethoxy]-ethoxy)-1,4-bis(3,4,5-trimethoxystyryl)benzene (3). Mp: 107−110 °C. HRMS (FAB, *m*/*z*): anal. calcd for $C_{76}H_{74}O_{14}$, 1210.5247; found, 1210.5079. ^{1}H NMR ($CDCl_3$): δ 2.15 (m, 4 H), 2.45 (t, 4 H, J = 8 Hz), 3.33 (t, 4 H, J = 8 Hz), 3.81 (t, 4 H, J = 4 Hz), 3.89 (overlapping s plus t, 20 H), 4.17 (t, 4 H, J = 8 Hz), 4.31 (t, 4 H, J = 4 Hz), 6.73 (s, 4 H), 6.99 (d, 2 H, J = 16 Hz), 7.29 (d, 2 H, J = 16 Hz), 7.06 (s, 2 H), 7.80 (d, 2 H, J = 8 Hz), 7.97 (m, 10 H), 8.12 (m, 8 H). ^{13}C NMR ($CDCl_3$): 26.70, 30.95, 32.20, 33.75, 56.12, 61.27, 63.35, 69.05, 69.45, 69.95, 103.69, 122.59, 123.35, 124.75, 124.87, 124.98, 125.10, 125.97, 126.63, 127.07, 127.34, 127.46, 128.68, 129.69, 129.90, 130.13, 131.36, 133.50, 135.72, 137.30, 150.92, 153.38, 173.41. UV−vis (THF, λ_{max}/nm [ϵ]): 243 [103800], 266 [41300], 277 [64500], 328 [61000], 344 [84550], 375 [32300].

(*E*,*E*)-2,5-Bis(4-(1-pyrenyl)butyryloxy)-1,4-bis(3,4,5-trimethoxystyryl)benzene (4). Mp: 224−226 °C. HRMS (FAB, *m*/*z*): anal. calcd for $C_{68}H_{58}O_{10}$, 1034.3668; found, 1034.4030. ^{1}H NMR ($CDCl_3$): δ 2.40 (m, 4 H), 2.82 (t, 4 H, J = 7.2 Hz), 3.53 (t, 4 H, J = 8 Hz), 3.67 (s, 12 H), 3.78 (s, 7 H), 6.61 (s, 4 H), 6.95 (d, 2 H, J = 16 Hz), 7.01 (d, 2 H, J = 16 Hz), 7.42 (s, 2 H), 7.92−8.12 (m, 20 H). ^{13}C NMR ($CDCl_3$): 26.98, 32.84, 33.97, 55.93, 60.95, 103.88, 120.21, 120.45, 123.18, 124.90, 125.10, 125.97, 126.93, 127.35, 127.44, 127.68, 128.75, 130.14, 130.83, 131.43, 131.87, 132.70, 135.02, 138.40, 145.89, 153.38, 171.54. UV−vis (THF, λ_{max}/nm [ϵ]): 243 [127000], 265 [57500], 277 [74400], 328 [62000], 344 [82000], 393 [42800].

Segmented Copolymer (5). Yellow powder. UV−vis (THF, λ_{max}/nm [ϵ]): 242 [67000], 264 [35500], 276 [48000], 315 [22600], 328 [40500], 344 [51300], 375 broad [10000]. GPC (THF): M_n = 9100, M_w = 15700. ^{1}H NMR ($CDCl_3$): δ 1.27−1.43 (m, 10 H), 1.75−1.92 (m, 14 H), 3.28 (m, 6 H), 3.62 (m, 4 H), 3.85 (m, 12 H), 3.94 (m, 6 H), 4.20 (m, 4 H), 6.62 (m, 2 H), 6.70 (m, 2 H), 7.03 (m, 2 H), 7.14 (s, 1 H), 7.30 (m, 2 H), 7.79−8.26 (m, 20 H). A small residuum of vinyl end group resonances was observed at δ 5.2−5.5 in the ^{1}H NMR. ^{13}C NMR ($CDCl_3$): 22,68, 25.30, 25.84, 28.33, 29.46, 29.76, 30.10, 31.61, 33.18, 34.68, 56.11, 69.32, 71.44, 73.59, 103.39, 103.83, 123.38, 124.79, 125.00, 125.76, 126.54, 127.19, 127.51, 128.58, 129.74, 130.88, 131.40, 133.03, 133.34, 136.85, 137.30, 151.09, 153.56.

(*E*,*E*)-2,5-Bis(2-hydroxyethoxy)-1,4-bis(3,4,5-trimethoxystyryl)benzene (11). This compound was made by a previously published[4] procedure. Mp: 245−247 °C. ^{1}H NMR (DMSO-d_6): δ 3.67 (s, 6 H), 3.82 (overlapping s plus t, 16 H), 4.08 (t, 4 H, J = 4 Hz), 6.89 (s, 4 H), 7.3 (d, 2 H, J = 16.8 Hz), 7.45 (d, 2 H, J = 16.8 Hz), 7.34 (s, 2 H).

(*E*,*E*)-2,5-Bis(undecanoloxy)-1,4-bis(3,4,5-trimethoxystyryl)-benzene (19). Mp: 103−105 °C. HRMS (FAB, *m*/*z*): anal. calcd for $C_{50}H_{70}O_{10}$, 830.4827; found, 830.4969. ^{1}H NMR ($CDCl_3$): δ 0.87 (t, 6 H, J = 6 Hz), 1.25 (m, 24 H), 1.43 (m, 4 H), 1.83 (m, 4 H), 2.64 (t, 4 H, J = 7.6 Hz), 3.87 (s, 8 H), 3.89 (s, 16 H), 6.69 (s, 4 H), 6.94 (d, 2 H, J = 16 Hz), 7.00 (d, 2 H, J = 16 Hz), 7.37 (s, 2 H). ^{13}C NMR ($CDCl_3$): 14.12, 22.68, 25.15, 29.30, 29.90, 31.88, 34.47, 56.11, 61.00, 64.80, 103.87, 120.14, 124.56, 127.35, 132.72, 138.43, 145.82, 153.41, 172.04. UV−vis (THF, λ_{max}/nm [ϵ]): 356 [24900].

SCHEME 1: Multichromophore Syntheses: (a) NaH, THF, Heat 7 days, 28%; (b) $Pd(OAc)_2$, P(*o*-tolyl)$_3$, DMF/NBu_3, 85-90 °C, 76%; (c) $Pd(OAc)_2$, P(*o*-tolyl)$_3$, DMF/NBu_3, 120-125 °C, 40%; (d) NEt_3, 24 h, 70%; (e) 2-butanone, K_2CO_3, 18-crown-6, Heat 7 days, 61%; (f) $Pd(OAc)_2$, P(*o*-tolyl)$_3$, DMF/NBu_3, 120 °C, 77%; (g) 12, CH_2Cl_2, NEt_3/DMAP, 40%; (h) $ClCH_2OCH_3$, HN(*i*-Pr)$_2$/CH_2Cl_2, 94%; (i) $Pd(OAc)_2$, P(*o*-tolyl)$_3$, DMF/NBu_3, 105 °C, 91%; (j) *p*-toluene sulfonic acid, r.t., EtOH/CH_2Cl_2, 84%; (k) 4-(1-pyreny))butyric acid, PPh_3/NEt_3/CCl_4, CH_3CN, 48 h, 56%.

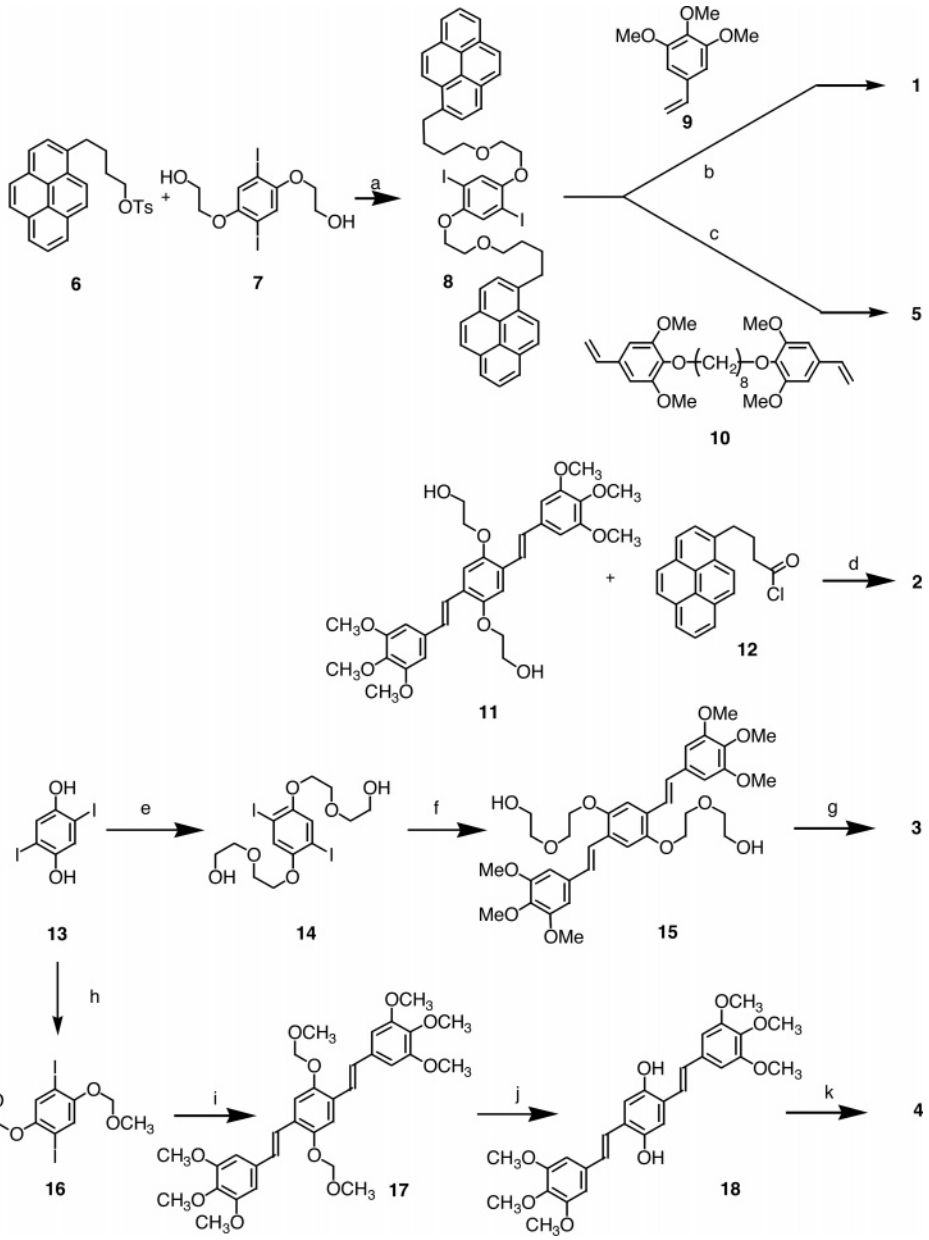

(*E*,*E*)-2,5-Bis(undecanoloxy)-1,4-bis(3,4,5-trimethoxystyryl)-benzene (19). Mp: 103−105 °C. HRMS (FAB, *m*/*z*): anal. calcd for $C_{50}H_{70}O_{10}$, 830.4827; found, 830.4969. ^{1}H NMR ($CDCl_3$): δ 0.87 (t, 6 H, J = 6 Hz), 1.25 (m, 24 H), 1.43 (m, 4 H), 1.83 (m, 4 H), 2.64 (t, 4 H, J = 7.6 Hz), 3.87 (s, 8 H), 3.89 (s, 16 H), 6.69 (s, 4 H), 6.94 (d, 2 H, J = 16 Hz), 7.00 (d, 2 H, J = 16 Hz), 7.37 (s, 2 H). ^{13}C NMR ($CDCl_3$): 14.12, 22.68, 25.15, 29.30, 29.90, 31.88, 34.47, 56.11, 61.00, 64.80, 103.87, 120.14, 124.56, 127.35, 132.72, 138.43, 145.82, 153.41, 172.04. UV−vis (THF, λ_{max}/nm [ϵ]): 356 [24900].

Results

Synthesis. Scheme 1 summarizes the methods used to make compounds **1**−**5**. Tosylate **6** was made[5] by reduction and tosylation of commercially available 4-(1-pyrenyl)butyric acid, then coupled with diol **7**[4] to make diiododiether **8**. Heck-type coupling of **8** with 3,4,5-trimethoxystyrene,[6] **9**, gave compound **1**. A similar procedure using divinyl compound **10**[7] gave segmented copolymer **5**. The etherification between **6** and **7** was sometimes problematic, so we switched to esterification for subsequent tether assemblies. A pre-assembled *para*-distyrylbenzene unit, **11**, was made by our previously reported route[4] and reacted with 4-(1-pyrenyl)butyryl chloride,[8,9] **12**, to give ester-tethered **2** in good yield and high purity. Similarly, 2,5-diiodohydroquinol **13**[5] was converted to diiodo-diol **14**[10] and coupled with styrene **9**[6] to give diol **15**, which was then esterified with **12**[8,9] to give **3**. Compound **13**[5] was also protected as the bis-methoxymethyl ether **16**, subjected to Heck coupling to give distyrylbenzene **17**, and deprotected to give the quinol **18**, which was esterified with **12** to give **4**. An alternative route to obtain **4** by first esterifying **13** with **12**, followed by Heck coupling with **15**, gave poor and variable yields, whereas the

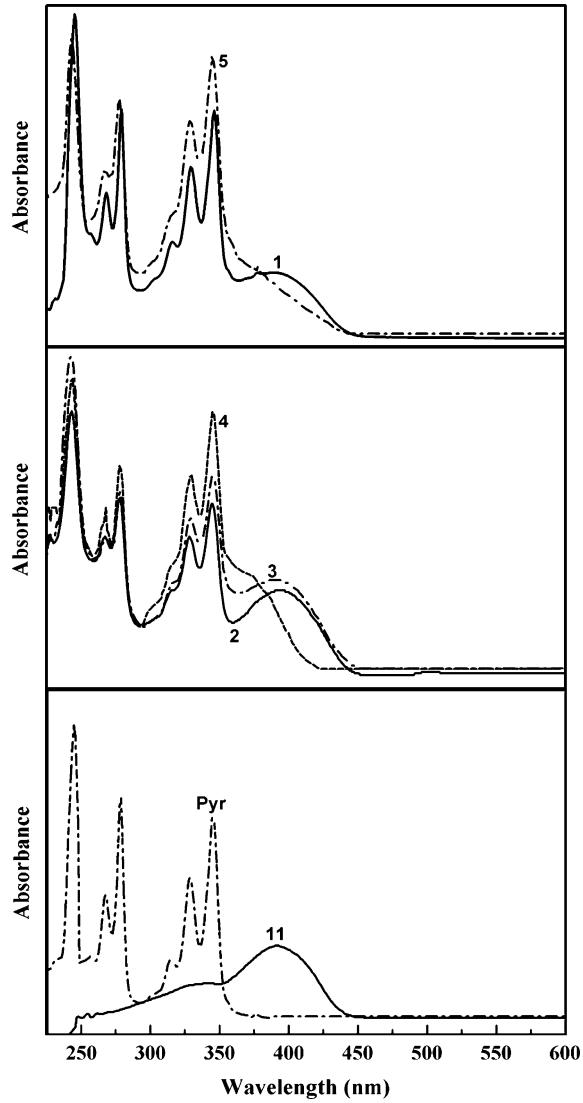

Figure 1. UV−vis spectra in chloroform of **1**−**5**, **11**, and pyrene (Pyr). Absorbances scaled for similarity in comparison.

route shown in Scheme 1 was dependable in our hands. The use of 4-(*N*,*N*-dimethylamino)pyridine (DMAP) significantly improved esterification yields by comparison to procedures without it.

Compounds **1**−**4** were characterized by ^{1}H NMR and ^{13}C NMR, and their identities confirmed by high-resolution mass spectrometry. The high trans olefin specificity from the Heck coupling reactions was shown by ^{1}H NMR spectroscopy, which showed no evidence of cis ethylenic protons in the 6−7 region of these products. Polymer **5** was also characterized by gel permeation chromatography of **5** in tetrahydrofuran against polystyrene standards, which gave $\bar{M}_n = 9100$ with a polydispersity index of 1.7 and degree of polymerization 8−13. The polymer formed homogeneous films when cast from solution onto glass.

Absorption and Excitation Spectroscopy. Solution UV−vis spectra for **1**−**5** (Figure 1) reflect an overlay of the component chromophores, with a higher energy region from the pyrene exhibiting sharp vibronic fine structure at 270−350 nm and a lower energy featureless band at about 390 nm from the core distyrylbenzene chromophore. Table 1 summarizes these absorption spectral results. While multichromophores **1**−**3** show core chromophore absorption maxima similar[4] to core model system **11**, system **4** exhibits a blue-shifted core absorption. This is attributable to **4** having an OC═O group directly attached to the core, whereas **1**−**3** have an $O(CH_2)_2$ group attached; the latter tether attachment is a minimal perturbation relative to model core system **11**. The effect of direct attachment of an OC═O group to the core was shown by bis-undecanoyl ester **19**, which also exhibits a blue-shifted absorbance maximum by comparison to **11**. The difference in absorption spectrum in **4** thus is not simply due to the use of a shorter tether by comparison to systems **1**−**3**.

TABLE 1: UV−Vis, Fluorescence Maxima in Different Solvents for Multichromophores and Related Compounds[a]

	UV−vi s (λ_{max}, nm)				Fluore scence (λ_{max}, nm)			
compound	MCH[b]	ACN[b]	THF[b]	CHL[b]	MCH	ACN	THF	CHL
1	387	390	386	391	445	448	447	448
	343	342	343.5	346				
	327	326.5	328	329				
			315	316				
	275	275.5	277	279				
2	394	394	394	393	445.5	447.5	446	448
	343	342	345	346				
	326	326.5	330	330				
			318	317				
	275.5	275.5	278	278				
3	388.5	392	393	392	448	452	446	452
	343	342	344	345				
	327	326.5	328	329				
	276	275.5	277	278				
4	367	368	369	368	445	476	450	450
	343	342	344	345	426			
	326.5	326.5	328	329				
	275	276	277	278				
5			375	373	446	450	447.5	451
			343	345				
			327.5	328.5				
			315	316				
			276	277.5				
11	384	385	383.5	387	445	448	444.5	447.5
19	359	358	358	360.5	444	470	451	450
					421			

[a] Fluorescence excitation at 276 nm. [b] MCH, methylcyclohexane; ACN, acetonitrile; THF, tetrahydrofuran; CHL, chloroform.

Polymer **5** also shows a difference in its core component absorption relative to **11**. Since there is no difference in the conjugation length or direct substitution pattern on **5** relative to **11**, the spectral change is most likely attributable to a conformational or aggregation effect. One possible conformational effect may be twisting of the core conjugation system due to effects of incorporating both pendant tethers and the in-chain polymethylene linkers in the polymer chains. There is little solvent effect on the absorption of **5**; if the blue shift relative to **11** is due to aggregation or chain folding, then the effect is not significantly solvent dependent.

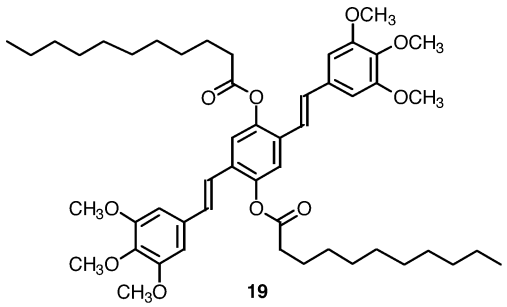

19

Fluorescence excitation spectra for **1**−**5** monitored at 445 nm match the corresponding absorption spectral bands well (see Supporting Information), supporting the absence of significant emitting impurities. By comparison, the excitation spectrum

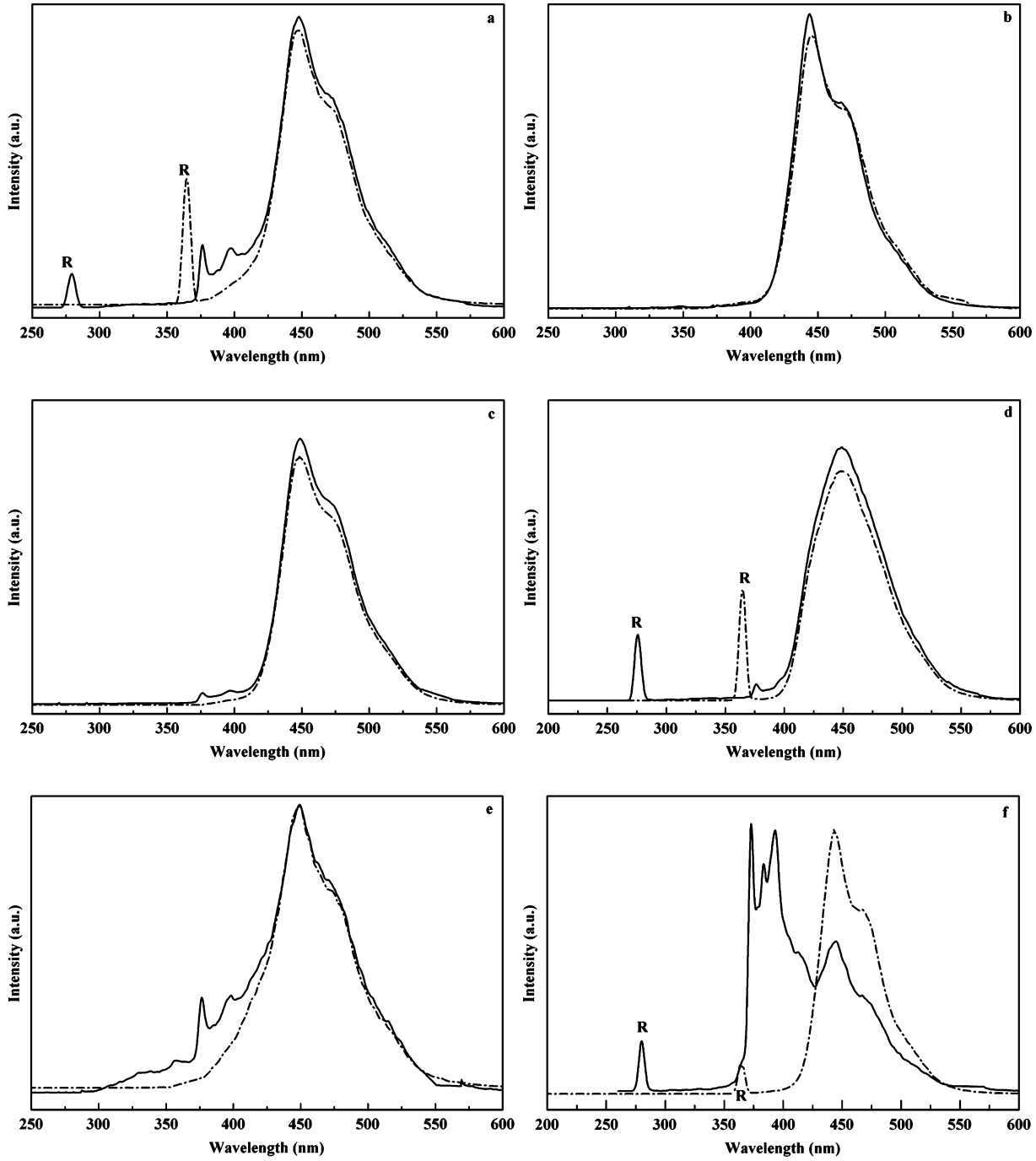

Figure 2. Emission spectra in chloroform of **1** (a), **2** (b), **3** (c), **4** (d), **5** (e), and a 2:1 mixture of pyrene:**11** (f); all at micromolar concentrations. Solid line spectra excited at 276 nm, and broken line spectra excited at 365 nm. Intensities in arbitrary units; ordinates in each plot are scaled relative to one another for ease of comparison. R = Rayleigh scattering peak.

monitored under the same conditions for a physical mixture of pyrene with core model chromophore **11** resembles the absorption spectrum of **11**, showing little energy transfer from pyrene to **11** under these low concentration (micromolar) conditions. These results will be further discussed below.

Emission Spectroscopy. Luminescence emission spectra were obtained for **1**−**5** at about 1 μM concentrations in chloroform using several excitation wavelengths. As a comparison to independent chromophore behavior, spectra were also obtained for 2:1 mixtures of pyrene:**11**. Example spectra for **1**−**5** are shown in Figure 2 for two excitation wavelengths, one for dominant pyrene absorption and one for dominant core absorption. Table 1 includes the emission spectral details. The multichromophores show nearly exclusive emission from the central core chromophores at about 445 nm (maximum) with some broadened vibronic features tailing to about 520 nm. The spectra are almost identical[4] to that of core model **11**. The remnant pyrene emission is a few percent at most and in some cases is undetectable despite excitation at wavelengths where pyrene has overwhelmingly dominant absorption. By comparison, spectra of the dilute physical mixture shows strong variation with excitation wavelength, showing that energy transfer from donor pyrene to acceptor **11** is limited at these concentrations.

Solvent effects in methylcyclohexane, tetrahydrofuran, chloroform, and acetonitrile are minimal for **1**−**3** and **5**. However, system **4** shows a significant luminescence solvent effect (Figure 3). Its emission spectrum in chloroform overlaps the spectra for **1**−**3** and **5** in chloroform but shows no vibronic features.

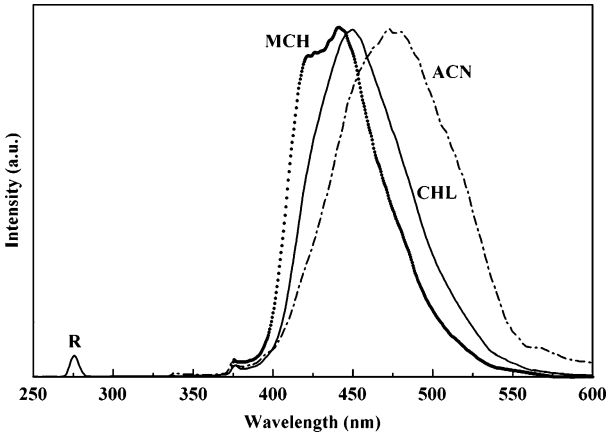

Figure 3. Solvatochromic effects on luminescence spectra of **4**. Intensities in arbitrary units; ordinates in each plot are scaled relative to one another for ease of comparison: MCH = methylcyclohexane, CHL = chloroform, ACN = acetonitrile, and R = Rayleigh scattering peak.

TABLE 2: Relative Fluorescence Emission Quantum Yields (Φ_{FL}) of Multichromophores and Related Compounds, Obtained in Tetrahydrofuran (THF) and Chloroform (CHL), with Estimated Energy Transfer Efficiencies, at 276 nm Excitation Wavelength (η_{ET})[a]

	Φ_{FL}		η_{ET}
Compound	THF	CHL	CHL
1	0.20	0.30	0.52
2	0.32	0.30	0.92
3	0.36	0.51	0.67
4	0.09	0.25	0.57
5	0.13	0.04	0.70
mixture	0.09	b	0.11
11	0.34	0.40	n/a
Pyrene	0.04	0.09	n/a

[a] See ref 3 for methodology. [b] Not determined.

In methylcyclohexane, vibronic features are visible, but the spectral maximum is blue shifted 30 nm relative to acetonitrile. The emission spectra of core model **19** show very similar behavior in the same solvents. The solvent shifts in **4** and **19** thus are attributed to the direct attachment of the π-polarizable OC═O group to the emitting chromophore, allowing a greater polarizability of their excited states. Despite this difference, energy transfer from excited-state pyrene antennae donors to the acceptor core in **4** still greatly dominates over pyrene emission.

The 1 μM physical mixtures of pyrene with **11** show emission from both chromophores until the excitation wavelength is increased to the point that **11** alone absorbs. For 276 nm excitation, the mixtures show much more pyrene emission relative to **11** in chloroform than in tetrahydrofuran (Supporting Information), whereas all the multichromophores show nearly exclusive core chromophore emission, regardless of solvent.

Quantum Yields. Solution-phase relative emission quantum yields ϕ_{fl} were measured[3] for **1**−**5**, pyrene, and core model chromophore **11** under the same conditions and are summarized in Table 2. The efficiency of energy transfer (η_{ET}) in **1**−**5** was estimated by a literature method[11] that compares normalized absorption and excitation spectra, assuming that the pendant pyrenes act as independent chromophores despite being tethered. The transfer efficiencies are also given in Table 2, with comparison to a 2:1 mixture of pyrene:**11** measured under the same conditions.

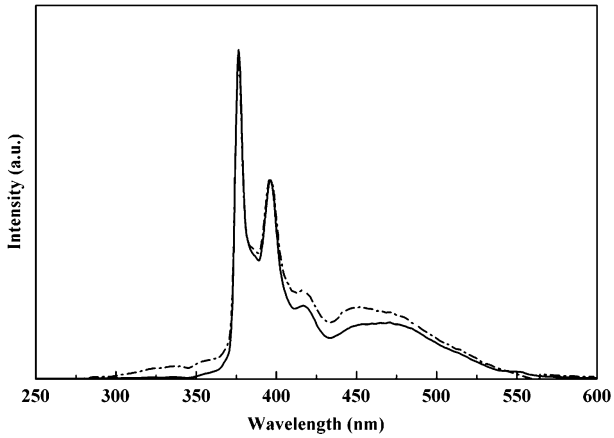

Figure 4. Emission spectra in chloroform of pyrene dyad model, **8**: solid line at 4 μM, broken line at 7500 μM. Ordinates in each plot are scaled relative to one another for ease of comparison.

Discussion

The pyrene fluorescence emission bands at about 400 nm (3.1 eV) are a good match for direct energy transfer to the distyryl benzene (2.5-oligo-PPV) acceptor core chromophore having UV−vis absorption about 385 nm (3.2 eV). When the core is excited, it emits at about 455 nm (2.7 eV). This antenna-to-core, donor-to-acceptor energy transfer mechanism is the main emission pathway for the multichromophores. Only a few percent of monomeric pyrene emission occurs in some cases (parts a, c, e of Figure 2) before energy transfer to the core.

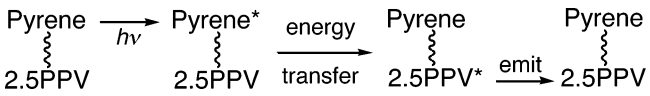

Pyrene excimer formation was not observed to occur to a significant extent in the multichromophores, judging by a lack of distortion of multichromophore emission spectra at millimolar concentrations by comparison to spectra of model core emitters **11** and **19**.

As a control for intramolecular excimer formation, the fluorescence emission of **8** was studied for excitation at <300 nm. In **8**, the pendant pyrenes are held within 30−32 Å (centroid−centroid distance) of one another, the same as in **1**−**2**. Pyrene itself shows predominantly monomeric emission in micromolar concentrations, with predominant (but not exclusive) excimer emission in millimolar concentrations.[12] Compound **8** shows significant monomer *and* excimer emission in similar ratios over 4−7500 μM concentrations (Figure 4), but its excimer emission intensity is 10-fold weaker than that of pyrene at millimolar concentrations and 40-fold weaker at micromolar concentrations than the emission bands observed for similar concentrations of **1**−**5** (all excited at 276 nm). The data support that neither intermolecular nor intramolecular pyrene excimer formation compete with pyrene to core energy transfer.

The quantum yields of Table 2 were obtained at excitation wavelengths where pyrene is essentially the sole absorber. Compounds **1**−**3** have similar quantum yields, while the short tethered system **4** and copolymer **5** have significantly smaller ones. A speculative but plausible reason for the lower quantum yield in the polymer is that chain folding may inhibit the ability of the pyrene antennae to achieve a favorable conformation for energy transfer. In the molecular multichromophores, the core is the energy sink with a reasonably high emission quantum yield and emission is favorable so long as overall concentrations are not large. However, in the copolymer, all the multichro-

mophores are tethered close to other multichromophores by the octamethylene linkers, providing far more quenching possibilities than those which occur for isolated multichromophores. If favorable conformations for energy transfer are hindered in **5**, then this would also explain why a more readily observable amount of pyrene emission occurs than in the molecular multichromophores (Figure 2e).

The reason for the poor quantum yield of **4** is less obvious but may be due to a tether that is too short to allow the pyrene antennae to adopt geometries favorable for energy transfer. The precise multichromophore geometry during the energy transfer is not known in this work. If a tethered pyrene is fully extended, then the distance from the central ring of the core to the pyrene centroid is 15−16 Å, but molecular mechanics calculations show that a pendant pyrene might stack above the alkoxy-substituted terminal rings of the core. Perfluorobenzene (PF) in ratios up to 8:1 PF:**2** was added in an effort to perturb the energy transfer process in **2** by intercalation into a putative stacked conformer but gave ≤2% decrease in emission intensity and no qualitative change in the spectrum. ^{1}H−-NOESY experiments for **2** in chloroform-*d* at ambient temperature (mixing times of 200, 300, 500, and 600 ms and 1.2 s) showed no significant interactions between the core chromophore methoxy groups and any of the pyrene C−H groups. This rules out significant conformational populations with a pyrene antenna closer than 5 Å to the terminal rings of the core. Of course, a very minor amount of a folded conformation may yield the observed energy transfer. Further work is required to evaluate what characteristics of the tether (rigidity, length, structure) can have a major influence on energy transfer properties of these multichromophores.

Because of the geometric flexibility of the multichromophores, it is not obvious whether dipole−dipole or direct orbital overlap models are most appropriate to describe the energy transfer process. For example, if intramolecular π-stacking of a pyrene pendant above the core assists energy transfer here, then that should favor the orbital overlap mechanism. Although recent studies[14] suggest that simple Förster or Dexter models have limitations when applied to some multichromophoric systems, the Förster approach is most typically used a priori. From the Förster model, a critical transfer distance parameter R_0 (in angstroms) can be obtained using eq 1,[13] where $J(\lambda)$ is evaluated by the overlap of the pyrene donor emission spectrum with the core absorbance spectrum, ϕ_D is the donor quantum yield, n is the medium refractive index, and $\kappa^2 = 0-4$ depending on the geometry of interaction between donor and acceptor dipoles. A value of $\phi_D = 0.04$ was measured for pyrene in chloroform (excitation at 345 nm), and $n = 1.446$ was used for the refractive index of chloroform at room temperature. By the use of the overlap between the pyrene emission and core (**11**) absorption spectra for $J(\lambda)$, the random orientation factor $\kappa^2 = 2/3$ yields a critical transfer radius of $R_0 = 25.4$ Å from eq 1. For collinear dipoles ($\kappa^2 = 1$) and collinear parallel dipoles ($\kappa^2 = 4$), $R_0 = 27.1$ Å and $R_0 = 34.2$ Å, respectively.

The structural framework of these Don → Acc ← Don multichromophores allows considerable mobility of the pyrene antennae/donors relative to the acceptor/emitter cores. The pyrene units can move from the geometric plane of the core to positions above the core, although the latter geometry is harder to attain for the short-tethered system **4**. Assuming completely random alignment orientations of pyrenes relative to cores may be an oversimplification, especially for **4**. The tethers in these systems are likely to constrain the pyrenes more to the plane of the core unit, to limit folding and resultant steric interactions for the relatively short tethers used in this study. This would tend to increase the orientation factor κ^2 above 2/3 but not to the upper limit of collinear parallel dipoles. If κ^2 is assumed to be 0.66−1.0, then the critical distance does not change much anyway, due to the one-sixth power dependence of R_0 on κ^2. Time-resolved tests such as fluorescence anisotropy experiments could shed more light on possible nonrandom dipole motion on the time scale of such tethered systems but are not available to us at present. We hope to be able to do this in the future.

$$R_0 = 0.211[\kappa^2 n^{-4} \phi_D J(\lambda)]^{1/6} \quad (1)$$

The energy transfer efficiencies η_{ET} from the antennae to the core are very good by comparison to physical mixtures of pyrene and **11** at the same concentrations. The optimal system is **2**, with a tether length of eight atoms through an ester linkage. The high efficiency in **2** is also shown by the fact its pyrene emission is nearly undetectable when excited, while the other multichromophores show varying small pyrene emission peaks. The ability to optimize efficiency as a function of the tunable tether is a desirable feature of these structurally simple multichromophores, which in principle can incorporate a wide variety of tether lengths, structures, and rigidities.

Summary

Multichromophores **1**−**4** have a structurally and synthetically simple design that provides a high local effective concentration of the pyrene antenna absorbers in the vicinity of the core acceptor chromophores, by tethering the chromophores together. Thus, energy transfer to the acceptor is much more efficient than that in a physical mixture at comparable concentration. Because a high effective concentration is achieved with a small real concentration, intermolecular quenching mechanisms such as pyrene excimer formation are much less important. Variation of the tethers not only allows for different degrees of "reining in" the energy gathering antennae to the core but also allows for solubility tuning in different solvents (e.g., water with PEG tethers). The synthetically tempting direct attachment of an ester unit to the core chromophore gave spectral variability with solvent and reduced the quantum yield in **4**, whereas putting the ester group in the middle of the tether did not perturb the energy transfer behavior significantly. This shows that tether tuning is important to find the best structure for energy transfer in this system. Also, too much antenna/core interlinking reduces overall energy transfer efficiency, judging by the presence of pyrene emission in polymer **5** and its reduced emission quantum yield. Future studies are planned to determine the effects of tether rigidification and structural alteration on energy transfer by comparison to the present set of systems **1**−**4** and hopefully time-resolved spectroscopy to probe the dynamics of the energy transfer processes as a function of structural change.

Acknowledgment. This work was supported in part by the University of Massachusetts College of Natural Sciences and Mathematics. We thank Prof. F. E. Karasz for use of a fluorimeter and Dr. L. Charles Dickinson for assistance with NOESY experiments.

Supporting Information Available: Comparison of pyrene emission to absorption of **11**, excitation spectra of **1**−**5**, comparison of absorption and excitation spectra for **1** and **2**, solvent dependence of fluorescence spectra for physical mixtures of pyrene and **11**, solvent dependence of fluorescence spectra for **19**, molecular mechanics optimized structure of **1**, 2D NOESY spectrum of **1**, and synthetic details for Scheme 1 (12 pages) are given. This material is available free of charge via the Internet at http://pubs.acs.org.

References and Notes

(1) (a) Weil, T.; Reuther, E.; Beer, C.; Muellen, K. *Chem.−Eur. J.* **2004**, *10*, 1398. (b) Tinnefeld, P.; Weston, K. D.; Vosch, T.; Cotlet, M.; Weil, T.; Hofkens, J.; Muellen, K.; De Schryver, F. C.; Sauer, M. *J. Am. Chem. Soc.* **2002**, *124*, 14310. (c) Wurthner, F.; Sautter, A. *Org. Biomol. Chem.* **2003**, *1*, 240. (d) Jenkins, R. D.; Andrews, D. L. *J. Chem. Phys.* **2003**, *118*, 3470. (e) Hu, B.; Karasz, F. E. *J. Appl. Phys.* **2003**, *93*, 1995. (f) Dai, Z.; Daehne, L.; Donath, E.; Moehwald, H. *J. Phys. Chem. B* **2002**, *106*, 11501. (g) Andrews, D. L. *Proc. SPIE Int. Soc. Opt. Eng.* **2002**, *4806*, 181. (h) Levitsky, I. A.; Krivoshlykov, S. G.; Grate, J. W. *J. Phys. Chem. B* **2001**, *105*, 8468.

(2) (a) Yang, Z.; Sokolik, I.; Karasz, F. E. *Macromolecules* **1993**, *26*, 1188. (b) Hu, B.; Karasz, F. E.; Morton, D. C.; Sokolik, I.; Yang, Z. *J. Lumin.* **1994**, 2022. (c) Yang, Z.; Hu, B.; Karasz, F. E. *Macromolecules* **1995**, *28*, 6151. (d) Gurge, R. M.; Hickl, M.; Krause, G.; Lahti, P. M.; Hu, B.; Yang, Z.; Karasz, F. E. *Polym. Adv. Technol.* **1998**, *9*, 504. (e) Pasco, S. T.; Lahti, P. M.; Karasz, F. E. *Macromolecules* **1999**, *32*, 6933. (f) Zheng, M.; Sarker, A. M.; Gürel, E. E.; Lahti, P. M.; Karasz, F. E. *Macromolecules* **2000**, *33*, 7426. (g) Sarker, A. M.; Gürel, E. E.; Zheng, M.; Lahti, P. M.; Karasz, F. E. *Macromolecules* **2001**, *34*, 5897. (h) Zheng, M.; Ding, L. M.; Gürel, E. E.; Lahti, P. M.; Karasz, F. E. *Macromolecules* **2001**, *34*, 4124. (i) Sarker, A. M.; Ding, L. M.; Lahti, P. M.; Karasz, F. E. *Macromolecules* **2002**, *35*, 223.

(3) Chen, Z.; Huang, W.; Wang, L.; Kang, E.; Chen, B.; Lee, C. S.; Lee, S. T. *Macromolecules* **2000**, *33*, 9015.

(4) Sierra, C. A.; Lahti, P. M. *Chem. Mater.* **2004**, *16*, 55.

(5) Winnik, F.; Winnik, M.; Tazuke, S.; Ober, C. *Macromolecules* **1987**, *20*, 38.

(6) Gangjee, A.; Devraj, R.; Queener, S. F. *J. Med. Chem.* **1997**, *40*, 470.

(7) Pasco, S.; Lahti, P. M.; Karasz, F. E. *Macromolecules* **1999**, *32*, 6933.

(8) Winnik, M. A.; Redpath, T.; Richards, D. H. *Macromolecules* **1980**, *13*, 328.

(9) Tran, C. D.; Fendler, J. H. *J. Am. Chem. Soc.* **1980**, *102*, 2923.

(10) Zhou, Q.; Swager, T. *J. Am. Chem. Soc.* **1995**, *117*, 12593.

(11) Devadoss, C.; Bharathi, P.; Moore, J. S. *J. Am. Chem. Soc.* **1996**, *118*, 9635.

(12) (a) Birks, J. B. *Rep. Prog. Phys.* **1975**, *38*, 903. (b) Birks, J. B. *Organic Molecular Photophysics*; John Wiley and Sons: Bristol, U.K., 1975.

(13) (a) Förster, T. *Discuss. Faraday Soc.* **1959**, *27−28*, 7. (b) Van Der Meer, B.; Coker, G. I.; Simon Chen, S. Y. *Resonance Energy Transfer: Theory and Data*; VCH Verlog: Weinheim, Germany, 1994. (c) Lakowicz, J. R. *Principles of Fluorescence Spectroscopy*; Plenum Publishers: New York, 1999. (d) Dale, D. E.; Eisinger, J.; Blumberg, W. E. *Biophys. J.* **1979**, *26*, 161.

(14) (a) Wong, K. F.; Bagchi, B.; Rossky, J. *J. Phys. Chem. A* **2004**, *108*, 5752. (b) Murphy, C. B.; Zhang, Y.; Troxler, T.; Ferry, V.; Martin, J. J.; Jones, W. E. *J. Phys. Chem. B* **2004**, *108*, 1537. (c) Harcourt, R. D.; Scholes, G. D.; Ghiggino, K. P. *J. Chem. Phys.* **1994**, *101*, 10521. (d) Seth, J.; Vaithianathan, P.; Johnson, T. E.; Prathapan, S.; Lindsey, J. S.; Bocian, D. F. *J. Am. Chem. Soc.* **1994**, *116*, 10578. (e) Metivier, R.; Kulzer, F.; Weil, T.; Müllen, K.; Basche, T. *J. Am. Chem. Soc.* **2004**, *126*, 14364.